

# The nucleation and growth of gold on silica

K. Luo<sup>a</sup>, D.Y. Kim<sup>b</sup>, D.W. Goodman<sup>a,\*</sup>

<sup>a</sup> Department of Chemistry, Texas A&M University, P.O. Box 30012, College Station, TX 77842-3012, USA

<sup>b</sup> Department of Chemistry, Hallym University, Seoul, South Korea

Received 9 June 2000

## Abstract

The nucleation and growth of Au clusters supported on SiO<sub>2</sub>/Mo(1 10) has been studied by X-ray photoelectron spectroscopy (XPS), low energy ion scattering (LEIS), and temperature programmed desorption (TPD). Stoichiometric ultra-thin SiO<sub>2</sub> films were synthesized and characterized by Auger electron spectroscopy (AES) and XPS. At 300 K, the growth mode of Au at fractional monolayer coverages is quasi-two-dimensional (2D); at higher coverages, three-dimensional (3D) growth was found with no evidence of a significant chemical interaction between gold and silica. Annealing Au/SiO<sub>2</sub>/Mo(1 10) to 1000 K led to sintering of the gold clusters. The desorption activation energies for Au coverages <0.2 monolayer equivalents were determined by TPD to be significantly lower than the sublimation energies found for higher coverages of Au clusters and for bulk gold. © 2001 Elsevier Science B.V. All rights reserved.

*Keywords:* Nucleation; Silica; Auger electron spectroscopy

## 1. Introduction

The surface chemistry and growth modes of metal clusters on oxides are issues fundamental to our understanding of the catalytic activity and selectivity of metal catalysts. Therefore, considerable research has addressed the physical and chemical properties of metal clusters on well-defined oxide surfaces [1–6]. Of special interest is that gold clusters of ca. 2–5 nm on certain oxides, e.g. titania, have been found to be very active catalysts for low temperature, selective oxidation [7,8]. Accordingly, Au on titania has received considerable recent attention [9–12], however, less attention has been directed towards other oxide supports. Transmission electron microscopy (TEM) and scanning tunnelling microscopy (STM) studies of

high coverages of Au on SiO<sub>2</sub> suggest that Au grows three-dimensionally [13–15]. Furthermore, X-ray photoelectron spectroscopy (XPS) indicates that the core level binding energies of Au clusters on silica increase significantly with decreasing particle size [1,16,17].

In this study, low energy ion scattered spectroscopy (LEIS) and XPS were used to study the initial growth of Au on ultra-thin SiO<sub>2</sub> film grown on Mo(1 10). Temperature programmed desorption (TPD) was used to estimate the bond strength of Au to SiO<sub>2</sub> and the influence of Au cluster size on the Au sublimation energy.

## 2. Experimental

The experiments were carried out in an ultra-high vacuum (UHV) chamber (base pressure of  $\sim 5 \times 10^{-10}$  Torr) equipped with XPS, Auger electron spec-

\* Corresponding author. Tel.: +1-979-845-0214;  
fax: +1-979-845-6822.  
E-mail address: goodman@mail.chem.tamu.edu (D.W. Goodman).

troscopy (AES), LEIS, low energy electron diffraction (LEED), and TPD.

The XPS data were collected using a Mg K $\alpha$  source (Perkin-Elmer) and a concentric hemispherical analyzer (PHI, SCA 10-360) aligned with the surface normal direction. LEIS experiments used a 650 eV He<sup>+</sup> beam with a scattering angle of 135°. To minimize ion beam damage, only one LEIS scan in the raster mode was used in each spectrum. AES, acquired with a primary electron beam energy of 3 kV, is reported in the  $d[N(E)]/dE$  mode. The TPD experiments were carried out using a close-coupled ( $\sim 1$  mm), line-of-insight quadrupole mass spectrometer (QMS) and a linear heating rate of 3 K/s.

The Mo(110) single crystal was spot-welded to high purity tantalum wires connected to two copper leads. The sample could be heated to 1500 K by resistive heating (2400 K by e-beam heating) and cooled to 90 K. The sample temperature was measured using a W-5% Re/W-26% Re thermocouple spot-welded to the back of the crystal. The Mo substrate was cleaned by repeated cycles of annealing at 1800 K in  $1 \times 10^{-7}$  Torr of O<sub>2</sub>, with a subsequent flash to 2300 K until no contamination was detected by AES, and a sharp hexagonal LEED pattern was evident.

Ultra-thin SiO<sub>2</sub> films were synthesized by exposing Mo(110) at 550 K to Si vapor in a  $1 \times 10^{-5}$  Torr O<sub>2</sub> background followed by an anneal to 650 K in background O<sub>2</sub>. The SiO<sub>2</sub> film was then characterized by AES, XPS, and LEED, and found to be stoichiometric and amorphous. The film thickness was measured using the attenuation of the Mo 3d (1020 eV) photoelectrons generated by a Mg K X-ray source, assuming a photoelectron mean free path of 23 Å [18].

Au was evaporated from a custom-built doser consisting of a high-purity Au wire (99.99%) wrapped around a tungsten filament. The gold wire was melted in UHV and thoroughly degassed prior to use. Since Au has been shown to grow on Mo(110) in a layer-by-layer growth mode (Frank van de Merwe mode) [19], AES and TPD were used to calibrate the Au dosing rate. In Fig. 1(a), the Au (69 eV)/Mo (186 eV) AES ratios from the differential AES spectra are plotted as a function of the Au deposition time. The linearity of the data in Fig. 1(a) and the apparent break in the plot indicate a layer-by-layer growth

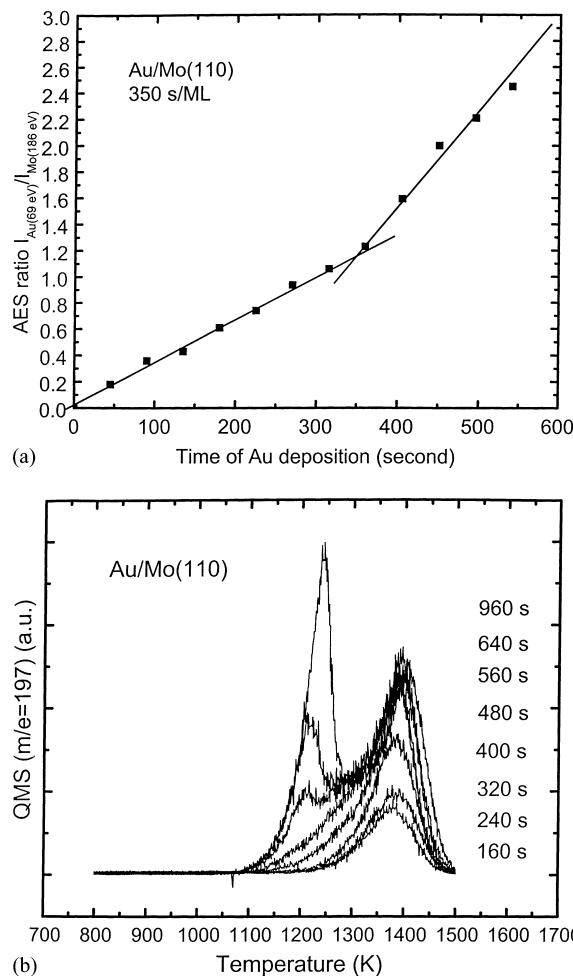


Fig. 1. Au dosing rate calibration: (a) Au (69 eV)/Mo (186 eV) AES signal ratio as a function of Au deposition time; (b) TPD spectra as a function of Au deposition time.

mode with an Au dosing rate of one monolayer (ML) per 350 s. Fig. 1(b) shows TPD spectra of Au desorption from a Mo(110) surface with two apparent desorption states of Au. The first feature at  $\sim 1250$  K corresponds to desorption from the first Au layer. The second feature between 1100 and 1300 K exhibits common leading edges with zero-order desorption kinetics, and is assigned to second layer desorption [19]. These TPD results are consistent with a dosing rate corresponding to completion of the first monolayer of Au between 320 and 400 s, in agreement with the AES results.

### 3. Results and discussion

#### 3.1. Synthesis of SiO<sub>2</sub> ultrathin films

AES (the Si LVV region) of the SiO<sub>2</sub> film growth sequence in Fig. 2 shows two Si oxidation states. In spectrum (a), the features at 92 and 107 eV correspond to Si<sup>0</sup> upon initial deposition of silicon. In spectrum (b), the three features at kinetic energies of 59, 63, and 76 eV indicate fully oxidized Si<sup>4+</sup> in the films, in agreement with previous studies [20,21]. The absence of an 85 eV feature rules out a SiO species. Growth of silica films at 550 K in a  $1 \times 10^{-6}$  Torr O<sub>2</sub> background yielded two Si oxidation states, Si<sup>4+</sup> and Si<sup>0</sup>, in XPS (not shown). The feature at 103.9 eV is assigned to the Si<sup>4+</sup> state and the second at 99.5 eV, to Si<sup>0</sup> [22–25]. Films grown at 550 K in  $1 \times 10^{-5}$  Torr O<sub>2</sub> and subsequently annealed to 650 K for 5 min gave a single feature at 103.9 eV, indicating exclusively Si<sup>4+</sup>; little oxidation of the Mo substrate was implied by XPS. This and previous studies [18,20,21] demonstrate that stoichiometric SiO<sub>2</sub> thin films can be synthesized on

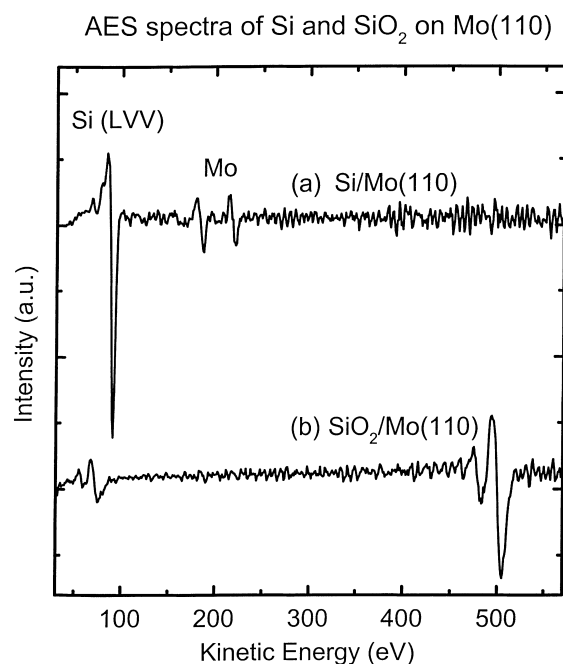


Fig. 2. (a) AES spectrum of silicon (Si) film ( $\sim 7$  Å) on Mo(110) surface; (b) AES spectrum of silica (SiO<sub>2</sub>) film ( $\sim 50$  Å) on Mo(110) surface.

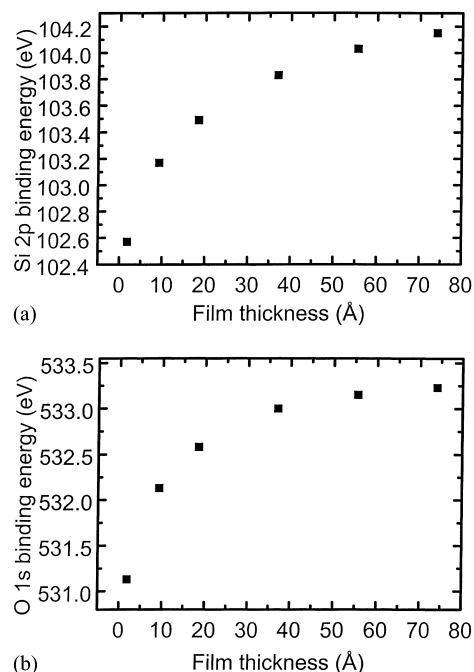


Fig. 3. Si 2p (a) and O 1s (b) binding energy of SiO<sub>2</sub>/Mo(110) as a function of SiO<sub>2</sub> film thickness.

Mo(110) with no evidence of any mixing between the silica films and the Mo substrate.

In Fig. 3(a) and (b), the Si 2p and O 1s binding energies are plotted as a function of film thickness. As the film thickness increases from  $\sim 2$  to 7 Å, the binding energy of the Si 2p feature increases by 1.6 eV and the O 1s by 2.0 eV. No binding energy shift is observed for the Mo 3d peak. Binding energy shifts of the Si 2p and O 1s as a function of SiO<sub>2</sub> film thickness have been reported [22,24,26] and attributed to charging within the film [22,27]. For example, in a previous study [25] the onset of charging of a SiO<sub>2</sub> film occurred at a film thickness of 17 Å. Similarly, the XPS results in Section 3.4 show strong evidence of charging.

Extra-atomic relaxation (screening) can also contribute to binding energy shifts [24]. During photoemission, electrons in higher energy levels in surrounding atoms relax into the positive hole. Lower binding energies (or higher kinetic energies) of the photoelectrons are a result of this relaxation. For a thin film, due to its relatively high conductivity, the Mo substrate

can contribute significantly to the screening effect of the oxide film along with relaxation within the film itself. Most atoms detected by XPS are from the surface layers whose positive holes are less screened by the Mo substrate and more so by the film itself. Therefore, positive binding energy shifts for Si 2p and O 1s are a consequence of increasing film thickness.

A Schottky barrier can form at the interface between the silica and the Mo substrate, and cause band bending in a thin silica film [28,29]. The conduction and valence bands of the film are destabilized, thus the Si and O core level peaks shift to lower binding energy. Since the distortion of the band extends only for a limited distance into the oxide film, the binding energy shift is more pronounced for relatively thin films [29]. With thicker films, the band bending contribution to the binding energy is smaller.

### 3.2. Thermal stability of SiO<sub>2</sub> films on Mo(1 1 0)

XPS indicates that the SiO<sub>2</sub> film thickness decreases little upon annealing to 1300 K. The film begins to evaporate at 1400 K, and is completely removed from the Mo substrate at ~2000 K. In Fig. 4, the Si 2p and O 1s binding energies for an ~50 Å thick film are shown as a function of temperature. Both Si and O features shift to higher binding energy with increasing temperature (650–1350 K), likely to further oxidation and thus improved SiO<sub>2</sub> film quality, as previously reported [20,30]. In this study, annealing is necessary for complete oxidation and the formation of a stoichiometric SiO<sub>2</sub> film. The corresponding loss in film conductivity and screening with the accompanying enhanced charging, leads to higher binding energy shifts for the Si 2p and O 1s features.

No obvious binding energy shift or change in the full width half maximum (FWHM) of the Mo 3d feature is apparent upon annealing the film to 1400 K. The chemical interaction then between the Mo substrate and the SiO<sub>2</sub> film is implied to be minimal.

### 3.3. Growth of Au on SiO<sub>2</sub>/Mo(1 1 0)

Fig. 5(a) shows LEIS as a function of Au coverage on a silica film (~50 Å) at 300 K. Two features at kinetic energies of 264 and 379 eV are assigned to He<sup>+</sup> scattered from O and Si, respectively. Au deposition leads to the growth of a feature at 576 eV. In Fig. 5(b),

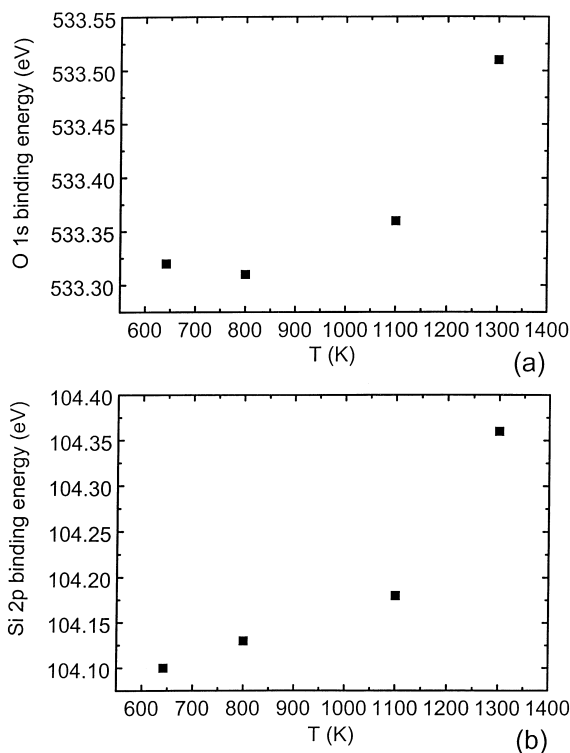


Fig. 4. O 1s (a) and Si 2p (b) binding energy of SiO<sub>2</sub> (~50 Å)/Mo(1 1 0) as a function of annealing temperature.

the area of the Au feature is plotted as a function of Au coverage. The linear relationship of the Au LEIS intensities with coverage suggests a quasi-two-dimensional (2D) growth at fractional monolayer coverages (below 0.10 ML). Subsequently, the Au feature increases slowly with a smooth, nonlinear relationship consistent with three-dimensional (3D) growth. Area plots of the Si and O features as a function of Au coverage are also consistent with the growth mode indicated above. Recent studies [9,11,12] have shown that Au growth is 2D at <0.1 ML on titanium oxide with an island structure related to the unique catalytic activity of Au/titania. The inhomogeneity of the silica film and surface charging makes STM studies at these coverages extremely difficult; however, further studies on more ordered structures will be very useful in providing more details regarding the nature of the growth mode.

To investigate the interfacial surface reaction and metal/substrate electronic properties, XPS experi-

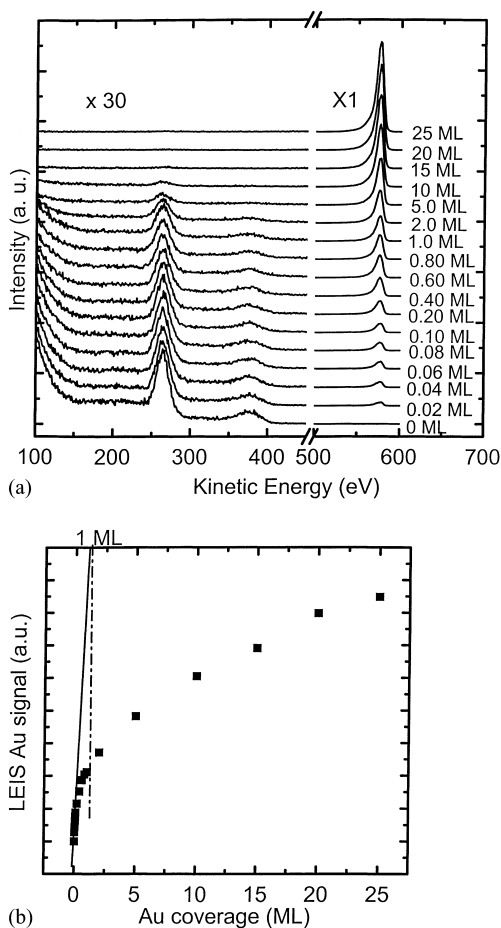


Fig. 5. (a) LEIS spectra of Au/SiO<sub>2</sub> (~50 Å)/Mo(110) at 300 K; (b) LEIS Au peak areas in (a) as a function of Au coverage.

ments were carried out for various Au coverages on SiO<sub>2</sub> (~50 Å) at 300 K. In Fig. 6(a), the Au 4f<sub>7/2</sub> binding energy, plotted as a function of Au coverage, shifts to higher binding energy as the Au coverage decreases. At an Au coverage of 0.02 ML, the Au 4f<sub>7/2</sub> core level binding energy is 1.6 eV higher than that of bulk Au with a corresponding increase in the Au 4f FWHM with decreasing Au coverage (not shown). Fig. 6(b) and (c) show plots of the Si 2p and O 1s core level binding energies as a function of Au coverage, respectively. At Au coverage of 0.02 ML, both Si 2p and O 1s binding energies decrease by 0.2 and 0.3 eV, respectively, with the shifts gradually decreasing with increasing Au coverage. Above an Au coverage of 0.5

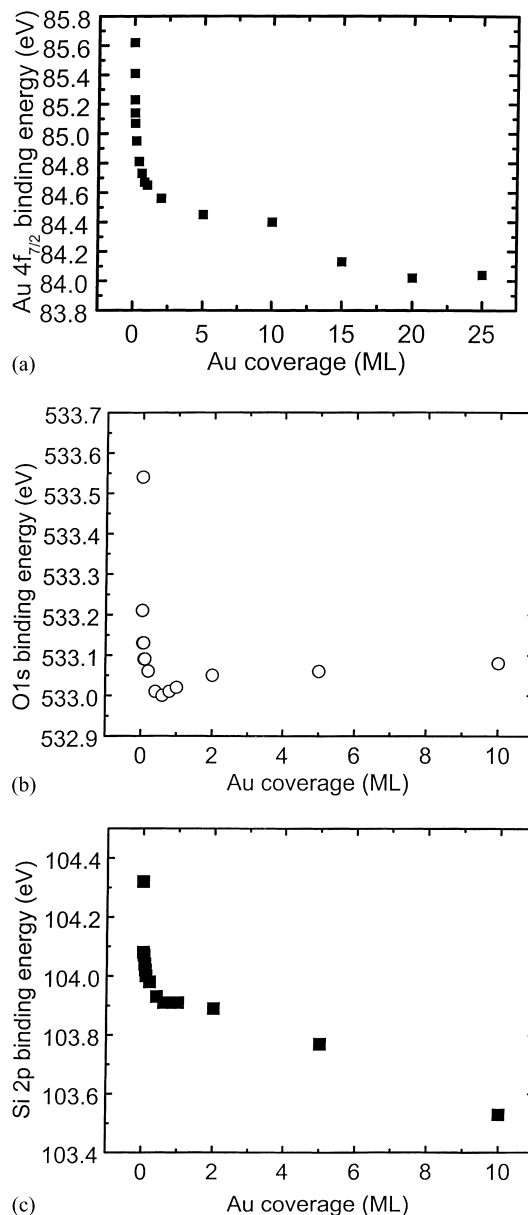


Fig. 6. (a) Au 4f<sub>7/2</sub> binding energy as a function of Au coverage at 300 K; (b) O 1s binding energy as a function of Au coverage; (c) Si 2p binding energy as a function of Au coverage.

ML, the Si 2p binding energy continues to decrease, however, the O 1s feature remains at ~533.0 eV. The Au core level binding energy shift as a function of coverage (Fig. 6(a)) illustrates the dependency of the

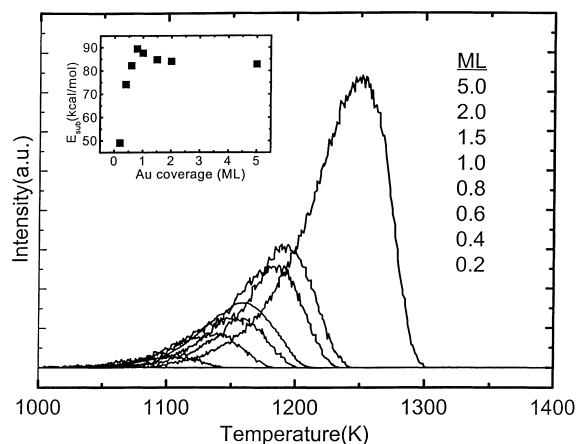


Fig. 7. TPD spectra of Au/SiO<sub>2</sub> (25 Å)/Mo(1 1 0) with different Au coverages. The insert is the Au sublimation energy as a function of Au coverage by leading edge analysis.

cluster electronic properties on size. Mason and Cox have reported similar results [1,16,17]. An increase of the Au 4f FWHM with decreasing Au coverage was found in the previous study as well. Initial and final state effects [9,31–34] that contribute to the peak shift and broadening are discussed in detail elsewhere [35]. Following Au deposition on the silica film, the Si 2p and O 1s binding energies shift to lower values with increasing Au coverage. This shift is due at least in part because of more effective screening from the larger Au clusters. These results are consistent with relaxation effects playing an important role in the Si 2p and O 1s binding energy shifts as a function of film thickness. With these considerations and the apparent lack of any change in the peak shape for the oxide or the metal XPS features, the chemical interaction between Au and SiO<sub>2</sub> at Au coverages >0.10 ML is presumed to be rather weak.

The interaction between Au clusters and the silica films was also studied by TPD. Fig. 7 shows a family of TPD spectra as a function of Au coverage. The leading edge of the peaks shifts continuously to higher temperature as the Au coverage increases. The insert in Fig. 7 shows the heat of sublimation ( $E_{\text{sub}}$ ), estimated from the desorption leading edge, as a function of Au coverage. At 0.2 ML Au coverage, the  $E_{\text{sub}}$  is ~50 kcal/mol, some 40 kcal/mol lower than the bulk value (~90 kcal/mol). This value increases rapidly with increasing Au coverage, finally reaching

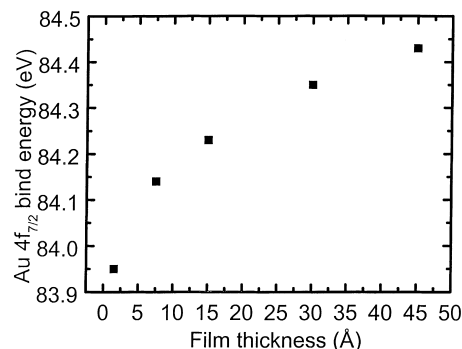


Fig. 8. Au 4f<sub>7/2</sub> binding energy upon 2.0 ML Au coverage as a function of film thickness.

the bulk value. A decrease in the average coordination number of Au atoms in the small clusters and a corresponding increase in the weaker Au–SiO<sub>2</sub> interactions most likely contribute to this attenuation of the sublimation energy [10,36–38].

### 3.4. Effect of silica film thickness on Au/SiO<sub>2</sub>/Mo(1 1 0)

The dependence of the Si 2p and O 1s binding energy shifts on film thickness has been discussed in Section 3.1. For a given Au coverage, XPS measurements were carried out to assess the influence of film thickness on the deposited Au. No binding energy shifts of the Si 2p and O 1s features are apparent with respect to Au coverage, however, the Au 4f binding energy does change with film thickness. In Fig. 8, the Au 4f<sub>7/2</sub> binding energy for a 2.0 ML Au coverage, plotted as a function of film thickness, increases with increasing film thickness. The Au 4f, Si 2p, and O 1s peaks also shift toward higher binding energy, whereas the Mo 3d feature remains unchanged. The Au 4f higher binding energy shift with increasing film thickness is consistent, with charging playing a substantial role in the Si 2p and O 1s core level binding energy shifts. Contributions to binding energy shifts related to changes in roughness of the silica film with thickness and consequent higher dispersion of the Au cannot be ruled out.

### 3.5. Annealing of Au/SiO<sub>2</sub>/Mo(1 1 0)

Sintering of metal clusters on oxide upon annealing has been reported for several metal/oxide systems

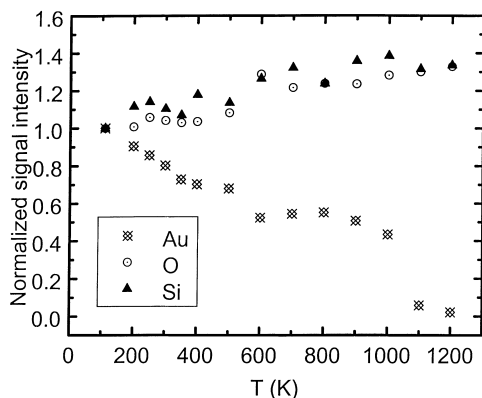


Fig. 9. Au, Si, and O normalized LEIS signals upon 0.2 ML Au coverage as a function of annealing temperature. The  $\text{SiO}_2$  film thickness is  $\sim 50 \text{ \AA}$ .

[9–11,35]. In this study, the LEIS peak area as a function of annealing temperature is plotted for an Au coverage of 0.2 ML in Fig. 9. The decrease in the Au intensity and the increase in the substrate intensity (both Si and O) indicate sintering of the Au clusters upon annealing. The sintering is more obvious from 100 to 600 K. After 600 K, the sintering slows until Au begins to evaporate above 1100 K. Similar results were obtained for several Au coverages.

Fig. 10 shows XPS data ( $\text{Au } 4f_{7/2}$  binding energy) as a function of annealing temperature for an Au coverage of 0.2 ML on  $\text{SiO}_2$  ( $\sim 50 \text{ \AA}$ ). No obvious shift ( $< 0.1 \text{ eV}$ ) is apparent from 100 to 1000 K. The Si 2p and O 1s core levels shift to higher binding energies

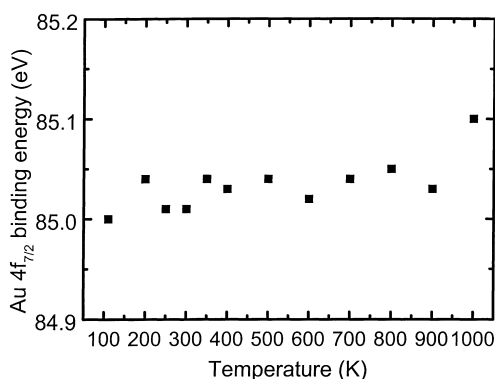


Fig. 10. Au  $4f_{7/2}$  binding energy upon 0.2 ML Au coverage as a function of annealing temperature. The  $\text{SiO}_2$  film thickness is  $\sim 50 \text{ \AA}$ .

with increasing temperature, as was observed for the clean film; annealing of various Au coverages showed similar results. More efficient screening within larger clusters formed via sintering should lead to a reduction in the Au 4f binding energy. In the present study, however, the Au 4f core level binding energy remains unchanged at low temperatures, and increases slightly at relatively high temperatures. This effect is most likely due to compensation of the enhanced screening by charging and/or a reduction in the support relaxation.

#### 4. Conclusions

Au growth on  $\text{SiO}_2/\text{Mo}(110)$  surface at 300 K was studied by LEIS and XPS. At  $< 0.10$  ML monolayer coverage, quasi-2D Au growth is observed. No strong chemical interaction is found between Au clusters and the silica film, or the silica film and the Mo substrate. XPS core level binding energy shifts are dependent on Au cluster size,  $\text{SiO}_2$  film thickness, and annealing temperature. Sintering of Au clusters is observed upon annealing. A marked decrease of the Au sublimation energy is apparent for small Au clusters.

#### Acknowledgements

We acknowledge with pleasure the support of this work by the Department of Energy, Office of Basic Energy Sciences, Division of Chemical Sciences, the Robert A. Welch Foundation, and the Dow Chemical Company. We also want to thank Dr. T.P. St. Clair and Dr. C.C. Chusuei for helpful discussions. D.Y. Kim acknowledges support by the Hallym Academy of Sciences, Hallym University, Korea.

#### References

- [1] M.G. Mason, Phys. Rev. B 27 (1983) 748.
- [2] C.T. Campbell, Surf. Sci. Rep. 27 (1997) 1.
- [3] D.W. Goodman, Surf. Rev. Lett. 2 (1995) 9.
- [4] D.R. Rainer, D.W. Goodman, J. Mol. Catal. A: Chem. 131 (1998) 259.
- [5] R. Persaud, T.E. Madey, in: D.A. King, D.P. Woodruff (Eds.), The Chemical Physics of Solid Surfaces and Heterogeneous Catalysis, Elsevier, Amsterdam, 1997.
- [6] V.E. Hendrich, P.A. Cox, The Surface Science of Metal Oxides, Cambridge University Press, Cambridge, 1994.

- [7] S.D. Lin, M. Bollinger, M.A. Vannice, *Catal. Lett.* 17 (1993) 245.
- [8] S. Lin, M.A. Vannice, *Catal. Lett.* 10 (1991) 47.
- [9] L. Zhang, R. Persaud, T.E. Madey, *Phys. Rev. B* 56 (1997) 10549.
- [10] C. Xu, W.S. Oh, G. Liu, D.Y. Kim, D.W. Goodman, *J. Vac. Sci. Technol. A* 15 (1997) 1261.
- [11] M. Valden, X. Lai, D.W. Goodman, *Science* 281 (1998) 1647.
- [12] S.T. Parker, A.W. Grant, V.A. Bondzie, C.T. Campbell, *Surf. Sci.* 44 (1999) 10.
- [13] L. Stockman, H. Vloeberghs, I. Heyvaert, C. Van Haesendonk, Y. Bruynseraede, *Ultramicroscopic* 42–44 (1992) 1317.
- [14] M. Arai, M. Mitsui, J.-I. Ozaki, Y. Nishiyama, *J. Colloid Interface Sci.* 168 (1994) 473.
- [15] A.A. Schmidt, H. Eggers, K. Herwig, R. Anton, *Surf. Sci.* 349 (1996) 301.
- [16] D.M. Cox, B. Kessler, P. Fayet, W. Eberhardt, Z. Fu, D. Sondericher, R. Sherwood, A. Kaldor, *Nanostructured Mater.* 1 (1992) 161.
- [17] D.M. Cox, W. Eberhardt, P. Fayet, Z. Fu, B. Kessler, R. Sherwood, D. Sondericher, A. Kaldor, *Z. Phys. D-Atoms Mol. Clusters* 20 (1991) 385.
- [18] J.-W. He, X. Xu, J.S. Corneille, D.W. Goodman, *Surf. Sci.* 279 (1992) 119.
- [19] S.H. Payne, H.J. Kreuzer, A. Pavlovskaya, E. Bauer, *Surf. Sci.* 345 (1996) L1.
- [20] X. Xu, D.W. Goodman, *Surf. Sci.* 282 (1993) 323.
- [21] X. Xu, D.W. Goodman, *Appl. Phys. Lett.* 61 (1992) 774.
- [22] T.L. Barr, *Appl. Surf. Sci.* 15 (1983) 1.
- [23] J.-W. He, X. Xu, J.S. Corneille, D.W. Goodman, *Surf. Sci.* 279 (1992) 119.
- [24] J. Finster, D. Schulze, F. Bechstedt, A. Meisel, *Surf. Sci.* 152/153 (1985) 1063.
- [25] T.J. Sarapatka, *J. Electron Spectrosc. Relat. Phenom.* 58 (1992) 233.
- [26] A. Ishizaha, S. Iwata, Y. Kamigaki, *Surf. Sci.* 84 (1984) 318.
- [27] T.L. Barr, *J. Vac. Sci. Technol. A* 7 (1988) 1677.
- [28] C. Kittel, *Introduction to Solid State Physics*, 6th Edition, Wiley, 1986.
- [29] Y. Wu, E. Garfunkel, T.E. Madey, *J. Vac. Sci. Technol. A* 14 (1996) 2554.
- [30] W.K. Choi, F.W. Poon, *J. Appl. Phys.* 81 (1997) 7386.
- [31] W.F. Egelhoff, *Surf. Sci. Rep.* 6 (1987) 253.
- [32] P.H. Citrin, G.K. Wertheim, *Phys. Rev. Lett.* 41 (1978) 1425.
- [33] F. Parmigiani, E. Kay, P.S. Bagus, *J. Electron Spectrosc. Relat. Phenom.* 36 (1985) 257.
- [34] P.S. Bagus, C.R. Brundle, G. Pacchioni, F. Parmigiani, *Surf. Sci. Rep.* 19 (1993) 265.
- [35] K. Luo, T.P. St. Clair, X. Lai, D.W. Goodman, *J. Phys. Chem. B* 104 (2000) 3040.
- [36] M.-C. Wu, D.W. Goodman, *J. Phys. Chem.* 98 (1994) 9874.
- [37] D.G. Van Campen, J. Hrbek, *J. Phys. Chem.* 99 (1995) 16389.
- [38] J.A. Rodriguez, M. Kuhn, J. Hrbek, *J. Phys. Chem.* 100 (1996) 18240.